Typhoons and Tigers—flood risk in the Sundarbans

S. F.-S. Need[1] A. V. Metcalfe[2] D. J. Sen[3]
P. K. Bhaskaran[4] M. F. Lambert[5]

(Received 28 February 2022; revised 26 July 2024)

Abstract

The many small inhabited islands of the Sundabarn region in north east India and Bangladesh, are subject to sea water flooding during cyclones. The objective is to predict flood risk so that improvements to flood defences can be prioritised. There are a few records of flood heights at a very limited set of locations, but there are long term data on cyclones that can be used to drive a simulation model to estimate flood risk at any points in the Sundarbans. The cyclone data is used to fit a stochastic model for cyclones. The cyclone model is combined with a deterministic storm surge model that provides sea level at the boundary of the Sundarbans. A hydraulic routing model, MIKE–21, is then used to predict water levels over a grid of interior points. The combined deterministic surge and routing models are approximated

DOI:10.21914/anziamj.v63.17196, Published 2024-08-07, as part of the Proceedings of the 15th Biennial Engineering Mathematics and Applications Conference. ISSN 1445-8810.

by a regression type model, so the stochastic simulation can quickly generate thousand of years of flood events. Results from a simulation are presented.

Contents

1 Introduction

The Sundarbans is a mangrove area in the delta formed by the confluence of the Ganges, Brahmaputra and Meghna rivers in the Bay of Bengal (Figure 1). Four protected areas in the Sundarbans are listed as UNESCO World Heritage sites and include tiger reserves. The Sundarbans is intersected by tidal streams and channels, and there are many small inhabited islands that are at risk of sea water flooding from cyclones in the Bay of Bengal. Earth bunds are built to provide rudimentary flood defences, but these will fail if overtopped by water. The objective of this research is to provide estimates of flood risk

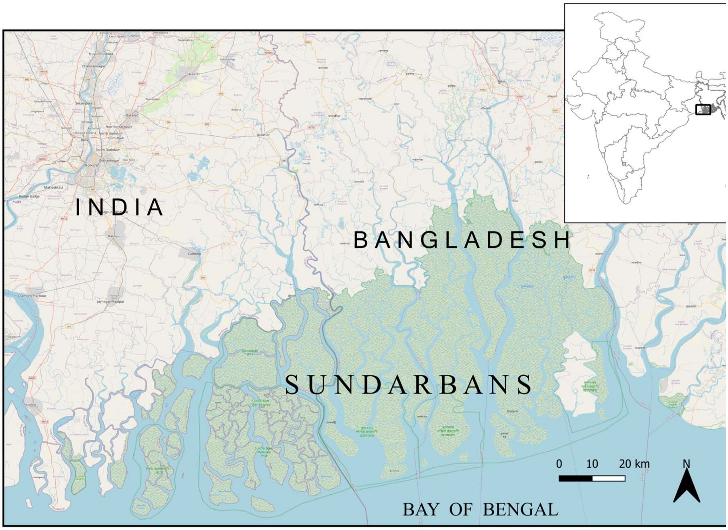

Figure 1: Sundarbans mangrove area in the north east of West Bengal and southern Bangladesh.

that can be used to plan the construction of improved flood defences or flood mitigation strategies.

We describe a stochastic simulation system that can provide estimates of flood risk at specified locations in the Sundarbans as follows.

- A stochastic model for cyclones generates starts of cyclone events, and for each cyclone event generates an origin point, track, and intensity.
- The Bay of Bengal Surge Model is a depth averaged hydrodynamic model that uses summary data from a generated cyclone to model the ensuing tidal surge at the ocean boundary of the Sundarbans.
- The tidal surge at the ocean boundary of the Sundarbans is added to the astronomic tide and provides boundary conditions for a hydrodynamic MIKE–21 model that models the increase in water level at any point in the Sundarbans.

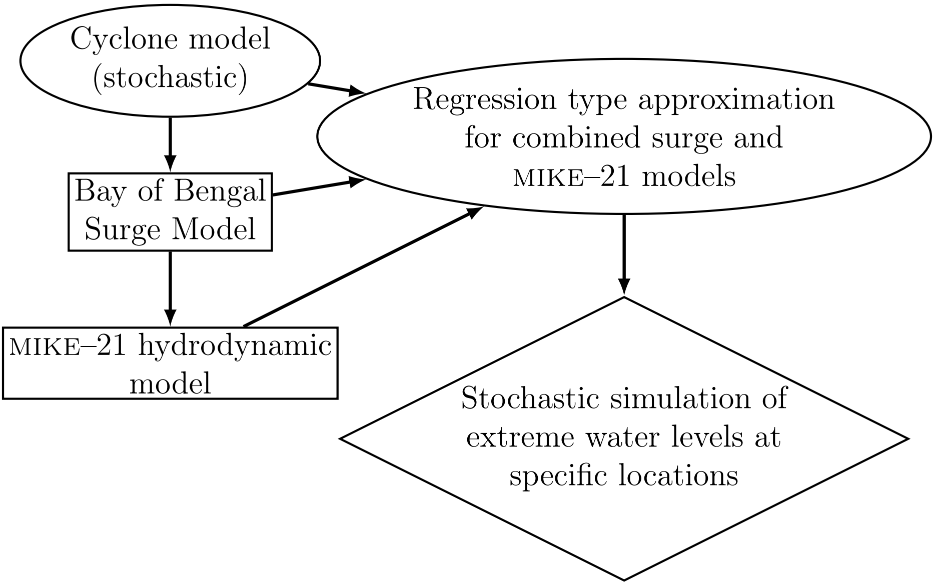

Figure 2: Strategy for simulating extreme water levels arising from cyclones. The regression type approximation replaces the combined hydrodynamic surge and MIKE–21 models.

- A regression type model is set up to predict the water level at some chosen point from features of the generated cyclone, obviating the use of computationally demanding deterministic hydrodynamic models.
- The regression type model is used to quickly generate extreme water levels over thousands of years.

The strategy is summarised in Figure 2.

2 Cyclone model

The Joint Typhoon Warning Centre (JTWC) has records of all storms with maximum sustained winds of at least 35 knots and which formed in the

North Indian Ocean from 1945 to the present. For this study, the suite of storms from 1971 to 2005 are used, these being the data of highest quality, which includes 244 storms formed in the Bay of Bengal, the region of the North Indian Ocean bordered by India to the West, Bangladesh to the North and Myanmar to the East. Of these storms, known as cyclones when they form over the Indian Ocean, information on the intensity, following the U.S. standard of maximum wind speed sustained over 1 minute at a height of 10 m above mean water level, is only available for 160 cyclones from 1972 onwards.

The rate of occurrence of cyclones is highly seasonal and the monthly rates (average number of storms per month), January through to December are: 0.20, 0.00, 0.03, 0.19, 0.88, 0.53, 0.26, 0.39, 0.57, 1.41, 1.63, 0.61. Moreover, the locations of the storm origins differ between monsoon and non-monsoon periods. Figure 3 shows storm origins during the monsoon in yellow (typically from May to September), and storm origins during the non-monsoon period are in red. Non-monsoon storm origins tend to lie south of the storm origins during the monsoon period. The movement of a cyclone is defined by its direction and tracking speed. Cyclones gain energy from passing over warm water, so storms which persist for long periods over the typically warm waters of the Bay of Bengal have more potential to collect energy, which in turn results in more intense cyclones (Figure 4). The intensity of a cyclone generally reduces once it makes landfall. However, the cyclone model is restricted to tracks of cyclones over the sea, and the salient features are as follows.

- Time varying Poisson model for occurrences.
- Mixed bivariate Gaussian model for genesis locations.
- A first order vector autoregressive model (abbreviated to VAR(1) model) for direction and speed of cyclone tracks. In this model the state vector is defined as deviations of direction and speed from the average. The state vector at time t is a linear combination of the two elements of the state vector at time $t-1$ and independent random variation with mean of zero.

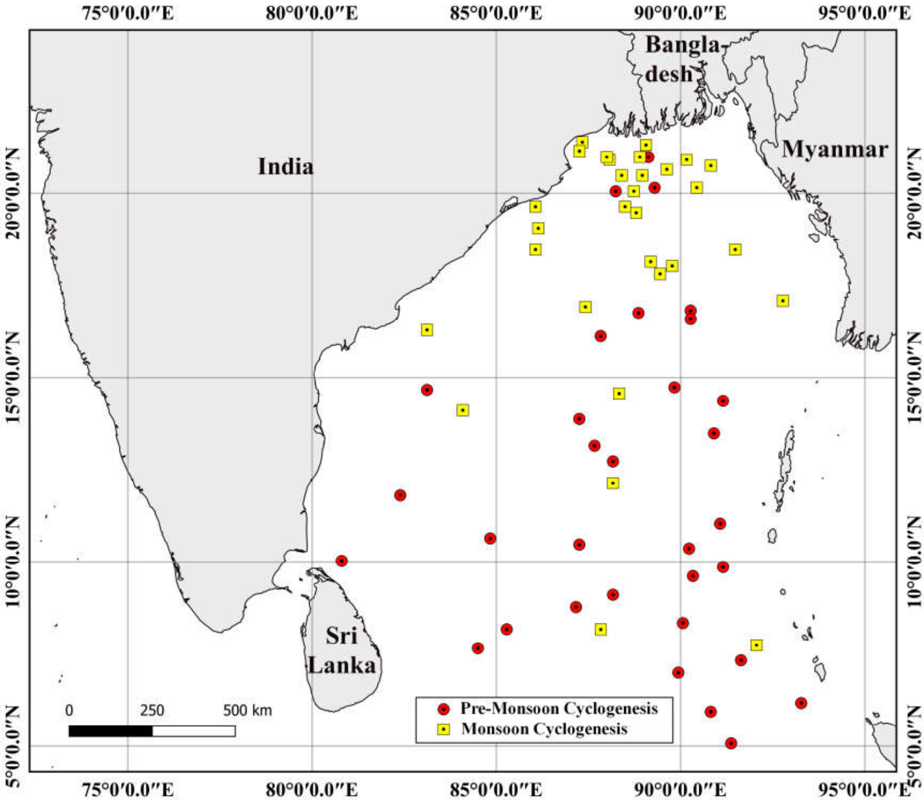

Figure 3: Genesis points of cyclones.

- An accept/reject procedure of a constant increase in rotation speed for cyclone intensities. That is, the rotation speed has a set probability of increasing by a constant amount and the complementary probability of being unchanged.

The International Best Track Archive for Climate Stewardship (IBTrACS) merges recent and historical tropical cyclone data from multiple agencies, including the JTWC, and would be preferred for future work.

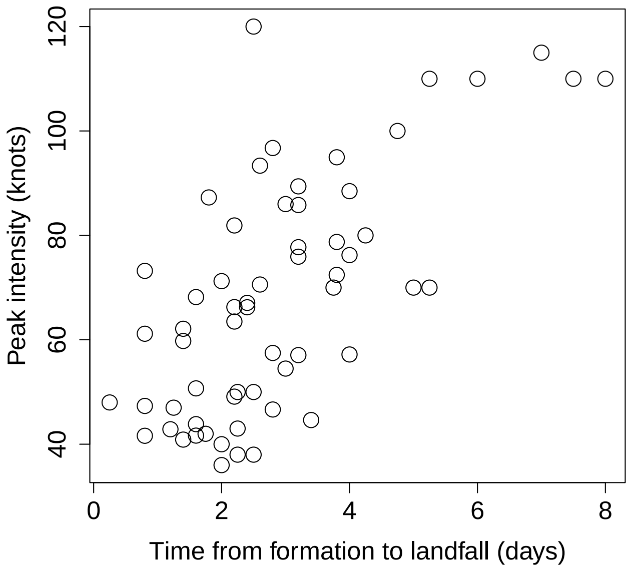

Figure 4: Cyclone intensity against duration.

3 Bay of Bengal Surge Model

A depth averaged 2D hydrodynamic model has already been developed for the Bay of Bengal (BB Surge Model) [2]. This model accepts an idealised cyclone of constant intensity moving along a cyclone track as input. This idealised cyclone is then represented as a wind shear stress acting on the water surface and as an atmospheric pressure drop located at the center of the cyclone. The boundary conditions for the model are set such that no flow is possible into or out from the coastal boundaries, and that open ocean boundaries may allow simple waves to exit the system, avoiding artificially introduced reflected waves from open ocean boundaries. The model extent is 1221 km EW by 532.8 km NS, represented by a grid of 331 by 154 pixels. The southern model boundary lies on the 18th parallel. The temporal resolution of the model is 60 s.

The model uses two closely related parameters to characterise the intensity of the storm: the radius of maximum winds; and the atmospheric pressure drop at the eye of the cyclone. As the JTWC does not record these data, it is necessary to evaluate these parameters from the maximum sustained wind speed (MSWS), which the JTWC does record. The conversion from the MSWS, denoted V_m, to the maximum atmospheric pressure drop is

$$\Delta p = CV_m^2\,, \tag{1}$$

where C is a constant of proportionality. The radius of maximum winds R_m is held constant at 20 km, as it has been found that the radius of maximum winds does not have a significant impact on the magnitude of the corresponding tidal surge. The calculation of wind stresses then follows from the pressure field, which is modelled as an exponentially decreasing field centred at the eye of the cyclone. The pressure at a distance r from the eye of the cyclone is

$$p(r) = p(\infty) - \Delta p \exp(-r/R_m)\,. \tag{2}$$

The wind speed at radius r is

$$V(r) = V(R_m)(r/R_m)^{3/2}\,. \tag{3}$$

The surface wind velocity field leads to the surface shear stresses which provide boundary conditions for simplified Navier–Stokes equations over a 2D fixed rectangular grid. Denote the x and y components of velocity by u and v, respectively, and the x and y components of shear stress as, respectively,

$$F = \rho c_D u(u^2 + v^2)^{1/2}\,, \quad G = \rho c_D v(u^2 + v^2)^{1/2}\,. \tag{4}$$

The BB Surge Model calculates storm surge levels at every grid point of the model and for every time step. For storm surge to be used as input into the more detailed hydraulic MIKE–21 model of the Sundarban region, the outputs of interest are the storm surge levels along the transect that matches the open ocean boundary of the MIKE–21 model.

4 MIKE–21 model

The MIKE-21 model is a two dimensional depth averaged hydraulic model, and Gayathri et al. [3] has already used it to model the mouth of the Hooghly River and much of the Sundarban region. The model region is nested inside that of the Surge Model. Our model is based on a grid of 949 EW by 441 NS pixels, covering a region of approximately 237 km by 110 km. The temporal resolution of the MIKE-21 model is 10 s. As the MIKE–21 model has a finer resolution than the BB Surge Model, in both space and time, the output from the BB Surge Model needs to be interpolated to provide sufficient boundary conditions for the MIKE–21 model. Linear interpolation is performed spatially prior to use in MIKE-21, whilst the temporal interpolations, which are also linear, are handled by MIKE–21. The MIKE–21 model allows for a more complex friction model to be incorporated, along with drying pixels, which are two important considerations when studying flooding of low lying islands. As the BB Surge Model does not incorporate the astronomical tide, only the tidal anomaly and the timing between tide and landfall is incorporated in the interpolation step. The MIKE–21 model is been calibrated against the limited flood level data available for Sagar Island.

5 Approximation and simulation

We refer to the combination of the deterministic BB Surge Model, astronomic tide, and MIKE–21 model as the hydraulic routing model (HRM). The input to HRM is a cyclone track and intensity, together with the astronomic tide, and the HRM output is the water depth at all pixels in the MIKE–21 model over time. The HRM takes several hours to run. Following Degenhardt et al. [1], the aim of the emulation model (EM) is to estimate the maximum water depth computed by the HRM at a specific pixel using a subset of the data input to HRM (Figure 5). The input to EM is: location of cyclone at landfall; tracking speed of cyclone at landfall; intensity of cyclone at landfall; and amplitude and phase of astronomic tide at landfall. For a given cyclone, the

EM model has five scalar inputs and a single scalar output and it could be implemented by a multiple regression (MR) or a neural network (ANN). The time to calculate a maximum water depth arising from a cyclone using a fitted MR or ANN is negligible.

We generate data for fitting a MR and ANN by selecting four cyclones from the JTWC library that are well documented and made landfall in the area modelled with MIKE–21. To ensure that the EM is used for interpolation rather than extrapolation, we construct a set of 100 cyclonic scenarios from the four observed cyclones by scaling the following observed features of each cyclone: the intensity defined as the maximum sustained wind speed; the tracking speed; the position of landfall; and the phase of the astronomic tide at time of landfall. Each of these features is scaled to, or set to, five different values. The intensity (V_o knots) is scaled to: 30, $(V_o+30)/2$, V_o, $(V_o+125)/2$, and 125. The tracking speed (s_o knots) is scaled by factors of 0.5, 0.67, 1, 1.5, and 2. The position of landfall could be 3, 4, 6, 9, and 12 fifteenths of the length of the sea boundary modelled with MIKE-21. The phase of the astronomic tide could be $-\pi/2$, $-\pi/4$, 0, $\pi/4$ and $\pi/2$. It is convenient to refer to the five values for each feature, in the given order, as very low (VL), low (L), mid (M), high (H), and very high (VH). For each observed cyclone, we consider 25 scaled versions: all 2^4 possible combinations of intensity, speed, landfall, and phase at L or H; 2×4 versions with three of the features set to M, with the fourth being VL or VH, and 1 version with all four features set at M. So, the set of 100 cyclonic scenarios consists of 25 versions of each of the four observed cyclones. Each scenario was run through the HRM, and so the MR and ANN could be fitted to 100 data 5-tuples. The coefficients of determination (proportion of the variance of the output explained by the model) for the MR, allowing quadratic terms and interactions, and the ANN, with 4 nodes and 2 layers, were 0.78 and 0.86, respectively, and the ANN was used for the simulation study. The point predictions from the ANN has a random draw from the distribution of residuals added to them, which allows for the uncertainty associated with the ANN prediction of the HRM output.

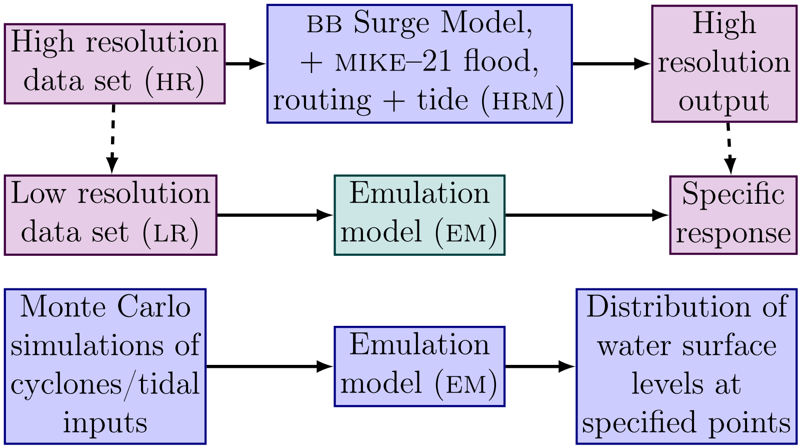

Figure 5: Simulation of cyclones and consequent water levels at specified points.

6 Results

6.1 Fitting the cyclone model

A Poisson regression including sinusoidal terms with periods of 1, 2, and 3 cycles per year is fitted to occurrence times of cyclones listed by JTWC, using a time step of one hour. The time varying rate parameter is

$$\begin{aligned}\lambda(t) = {} & 0.0007167 + 0.0005188 \times \cos(2\pi t/8766) - 0.0001112 \times \sin(2\pi t/8766) \\ & - 0.0001462 \times \cos(4\pi t/8766) - 0.0006299 \times \sin(4\pi t/8766) \\ & - 0.0000846 \times \cos(6\pi t/8766) + 0.0001033 \times \sin(6\pi t/8766)\,,\end{aligned}$$

where t is in hours, with $t = 0$ corresponding to midnight on 31st December, and 8766 being the number of hours in 365.25 days. In the simulation the probability of a cyclone occurring in a particular hour is given by λ, except when a simulated cyclone is in existence when the probability is set to zero. The possibility of cyclones merging, the Fujiwhara effect, is ignored.

The cyclone origins in the non-monsoon period are drawn from a bivariate

Gaussian distribution: of latitude and longitude with: means 10.12 and 90.08 degrees, standard deviations of 3.73 and 4.68 degrees, respectively, and correlation 0.09. The cyclone origins in the monsoon period were drawn from a bivariate Gaussian distribution of latitude and longitude with: means 19.09 and 88.94 degrees, standard deviations of 3.41 and 3.77 degrees, respectively, and correlation -0.23.

The fitted VAR(1) model for the movement of cyclones in the non-monsoonal period is modelled as

$$\begin{pmatrix} x_{1,t} \\ x_{2,t} \end{pmatrix} = \begin{pmatrix} 0.6752 & -0.1179 \\ -0.0301 & 0.6749 \end{pmatrix} \begin{pmatrix} x_{1,t-1} \\ x_{2,t-1} \end{pmatrix} + \begin{pmatrix} e_{1,t} \\ e_{2,t} \end{pmatrix},$$

where $x_{1,t}$ is direction, relative to the mean path of all non–monsoonal cyclones at time t in radians, and $x_{2,t}$ is the tracking speed, relative to the mean tracking speed of all non-moonsoonal cyclones at time t in degrees per hour. The $e_{1,t}$ and $e_{2,t}$ are zero mean serially uncorrelated random variations with variances of 0.32 and 0.31, respectively, and covariance of -0.03. The coefficients are obtained by fitting VAR(1) to individual cyclones and averaging the results. The corresponding model for the monsoonal period is

$$\begin{pmatrix} x_{1,t} \\ x_{2,t} \end{pmatrix} = \begin{pmatrix} 0.5310 & -0.1305 \\ -0.1514 & 0.7076 \end{pmatrix} \begin{pmatrix} x_{1,t-1} \\ x_{2,t-1} \end{pmatrix} + \begin{pmatrix} e_{1,t} \\ e_{2,t} \end{pmatrix},$$

where the $e_{1,t}$ and $e_{2,t}$ are zero mean serially uncorrelated random variation with variances of 0.67 and 0.44, respectively, and covariance of -0.15. The coefficients are obtained by fitting VAR(1) to individual cyclones and averaging the results.

The increase in intensity of the cyclone is modelled by

$$y_t = \begin{cases} y_{t-1} + 0.83 & \text{if } U < F(y_{t-1}+20)/\left[F(y_{t-1}) + F(y_{t-1}+20)\right], \\ y_{t-1} & \text{otherwise,} \end{cases}$$

where 0.83 is the increase in knots per hour, U has a Uniform distribution over $[0, 1]$, and $F()$ is the cdf of y.

Table 1: Maximum water level (m).

Period	0.05 quantile	median	0.95 quantile
30 years	7.9	11.1	14.5
15 years	7.0	9.6	12.2
10 years	6.5	8.6	10.0
5 years	6.0	7.1	8.3

Realisations from the cyclone model show close agreement with JTWC data, including features such as the distribution of points of landfall that are not explicitly incorporated in the modelling.

6.2 Simulation results

We present results for the pixel corresponding to the ocean side of the southernmost island in the Sundarbans (21.34 N, 88.87 W). The simulation proceeds as follows.

Step 1. Increment by one hour and check whether a cyclone is indicated. If not, then repeat.

Step 2. If a cyclone is indicated, then model its genesis point, track and intensity until it makes landfall. Store the landfall point, tracking speed and intensity.

Step 3. Generate a random phase and amplitude for the astronomic tide.

Step 4. Predict a maximum water level with the EM, and store.

Step 5. Increment by the duration of the cyclone and return to Step 1.

A simulation of $30,000$ years was run and partitioned into: 1000 consecutive 30 year periods; 2000 consecutive 15 year periods; 3000 consecutive 10 year periods; and 6000 consecutive 5 year periods. For each period the empirical distribution of the greatest values during the periods is obtained. The median, and lower and upper 0.05 quantiles are given in Table 1.

7 Discussion

The simulation procedure estimates the increase in water level from its mean level, as a function of average recurrence interval, at any location in the Sundarbans. Unfortunately, the mean water level is itself rising as a consequence of global warming. The measured mean global sea level rise has been 3.1 mm per year between 1993 and 2017 [5], but the increase in the Sundarbans has been estimated as closer to 10 mm per year, partly due to increasing siltation [4].

Acknowledgements SFN, AVM and MFL are grateful for invitations to visit IIT Kharagpur on several occasions whilst working on the project.

References

[1] A. Degenhardt, A. V Metcalfe, and S. Parsons. "Combined river and sea flooding". In: *34th MAFF Conference of River and Coastal Engineers, Keele University, 30 June to 2 July 1999*. 1999 (cit. on p. C245).

[2] S. K. Dube. "Prediction of storm surges in the Bay of Bengal". In: *Trop. Cyclone Res. Rev.* 1.1 (2012), pp. 67–74. DOI: 10.6057/2012TCRR01.08 (cit. on p. C243).

[3] R. Gayathri, P. K. Bhaskaran, and D. Sen. "Numerical study on storm surge and associated coastal inundation for 2009 AILA Cyclone in the head Bay of Bengal". In: *Aquatic Proc.* 4 (2015), pp. 404–411. DOI: 10.1016/j.aqpro.2015.02.054 (cit. on p. C245).

[4] A. F. Rahman, D. Dragoni, and B. El-Masri. "Response of the Sundarbans coastline to sea level rise and decreased sediment flow: A remote sensing assessment". In: *Remote Sen. Environ.* 115.12 (2011), pp. 3121–3128. DOI: 10.1016/j.rse.2011.06.019 (cit. on p. C250).

[5] WCRP Global Sea Level Budget Group. "Global sea level budget 1993–present". In: *Earth Sys. Sci. Data* 10.3 (2018), pp. 1551–1590. DOI: 10.5194/essd-10-1551-2018 (cit. on p. C250).

Author addresses

1. **S. F.-S. Need**, University of Adelaide, Australia.
   mailto:stevenfongsingneed@gmail.com
2. **A. V. Metcalfe**, University of Adelaide, Australia.
   orcid:0000-0002-7680-3577
3. **D. J. Sen**, Department of Civil Engineering, IIT Kharagpur, India.
4. **P. K. Bhaskaran**, Department of Ocean Engineering & Naval Architecture, IIT Kharagpur, India.
5. **M. F. Lambert**, School of Civil Engineering, University of Adelaide, Australia.